

A simple kinetic model for myeloma cell culture with consideration of lysine limitation

Yuan-Hua Liu · Jing-Xiu Bi · An-Ping Zeng ·
Jing-Qi Yuan

Received: 20 September 2007 / Accepted: 17 January 2008 / Published online: 6 February 2008
© Springer-Verlag 2008

Abstract A simple kinetic model is developed to describe the dynamic behavior of myeloma cell growth and cell metabolism. Glucose, glutamine as well as lysine are considered as growth limiting substrates. The cell growth was restricted as soon as the extracellular lysine is exhausted and then intracellular lysine becomes a growth limiting substrate. In addition, a metabolic regulator model together with the Monod model is used to deal with the growth lag phase after inoculation or feeding. By using these models, concentrations of substrates and metabolites, as well as densities of viable and dead cells are quantitatively described. One batch cultivation and two fed-batch cultivations with pulse feeding of nutrients are used to validate the model.

Keywords Myeloma cell line · Kinetic model · Amino acids · Lysine · Modeling · Growth kinetics

List of symbols

$C_{\text{Glc}}, C_{\text{Gln}}, C_{\text{Lac}}, C_{\text{Lys-ext}}, C_{\text{Lys-int}}$	concentrations of glucose, glutamine, lactate, extra- and intra-cellular lysine (g L^{-1})
$C_{\text{Glc,F}}, C_{\text{Gln,F}}, C_{\text{Lys-ext,F}}$	concentrations of glucose, glutamine, lactate, extra-cellular lysine in the feeding medium (g L^{-1})
$C_{\text{Lys-int0}}$	saturated level of intracellular lysine (g L^{-1})
F_i	flow rate of feeding (L h^{-1})
f_{max}	maximum specific uptake rate of extracellular lysine for filling the intracellular lysine pool [$\text{g} (\times 10^8 \text{ cell h})^{-1}$]
F_o	flow rate of sampling (L h^{-1})
k_1, k_2	parameters in the regulator model
K_f	saturated constant of extracellular lysine uptake for filling the intracellular lysine pool (g L^{-1})
k_{lys}	specific autolysis rate (h^{-1})
$K_{\text{Glc}}, K_{\text{Gln}}, K_{\text{Lys-int}}$	Monod constants (g L^{-1})
$m_{\text{Glc}}, m_{\text{Gln}}, m_{\text{Lys-ext}}$	maintenance coefficients of glucose, glutamine and extracellular lysine [$\text{g} (\times 10^8 \text{ cell h})^{-1}$]
$q_{\text{Glc}}, q_{\text{Gln}}, q_{\text{Lys-ext}}$	specific uptake rates of glucose, glutamine and extracellular lysine [$\text{g} (\times 10^8 \text{ cell h})^{-1}$]
q_{Lac}	specific production rate of lactate [$\text{g} (\times 10^8 \text{ cell h})^{-1}$]
$\mu_d, \mu_{d, \text{max}}$	actual and maximum specific death rate (h^{-1})

Y.-H. Liu · J.-Q. Yuan (✉)
Department of Automation, Shanghai Jiao Tong University,
800 Dongchuan Rd., 200240 Shanghai,
People's Republic of China
e-mail: jqyuan@sjtu.edu.cn

J.-X. Bi
School of Chemical Engineering,
The University of Adelaide, Adelaide, SA 5005, Australia

J.-X. Bi
Institute of Process Engineering,
Chinese Academy of Science,
100080 Beijing, People's Republic of China

A.-P. Zeng
Institute of Bioprocess and Biosystems Engineering,
Hamburg University of Technology (TUHH),
Denickestrasse 15, 21073 Hamburg, Germany

A.-P. Zeng
Research Group of System Biology,
Helmholtz Zentrum für Infektionsforschung, Inhoffenstraße 7,
38124 Braunschweig, Germany

K_d	death rate model parameter (h^{-1})
μ, μ_{\max}	actual and maximum specific growth rate (h^{-1})
μ_M, μ_R	specific growth rate obtained from Monod model and regulator model (h^{-1})
μ_{\min}	minimum specific growth rate in the regulator model (h^{-1})
v_0	single cell volume ($\times 10^{-11}$ L)
V	culture volume (L)
X_v	viable cell density ($\times 10^8$ cells L^{-1})
X_d	dead cell density ($\times 10^8$ cells L^{-1})
X_t	total cell density ($\times 10^8$ cells L^{-1})
$Y_{\text{Lac}/\text{Glc}}$	lactate yield on glucose (g g^{-1})
$Y_{\text{X}/\text{Glc}}, Y_{\text{X}/\text{Gln}}, Y_{\text{X}/\text{Lys}}$	cell number yields on glucose, glutamine and extracellular lysine ($\times 10^8$ cells g^{-1})

Introduction

Mathematical models of mammalian cell culture found in the literature vary widely in complexity and theoretical foundation, from the Monod model, to more sophisticated unstructured [1–3] and structured models [4–7]. Unstructured models are simple and therefore are attractive in applications [8–10], but they are of limited use in situations where significant changes in the cellular environment occur. Structured models can be used over a broader range of conditions and have better extrapolating capacity than unstructured ones, however, they may become too complex and computationally intensive for practical applications. The objective of this study is to develop a simple kinetic model which is the combination of the unstructured framework and part of the inner structures of the biological system.

Growth limiting or inhibiting factors, such as glucose and glutamine depletion, insufficient supply of other amino acids, the toxic byproducts ammonium and lactate, and the other probably not yet identified autocrine factors should be taken into account in modeling mammalian cell growth [2, 9, 11–14]. In cell culture, amino acids are used for energy production and protein synthesis. Importance of amino acids for in vitro mammalian cell growth has been confirmed in a number of publications [15–20]. Except for glutamine, amino acids are usually assumed to be supplied in excess so that they are not treated as limiting substrates in modeling. However, Robert and Hsu [21] found the significant lysine consumption (0.87×10^{-11} mol/cell h^{-1}) in myeloma cell culture. Martial-Gros et al. [19] revealed that lysine might be at limiting concentration in their serum containing medium for hybridoma cell culture. In our study, lysine was also found to be a limiting amino acid in myeloma cell culture. Therefore, the kinetic model proposed in this paper takes

lysine, glucose and glutamine as limiting substrates. In addition, the specific growth rate in a conventional unstructured model is usually formulated as Monod type kinetics [13, 22, 23]. However, such a Monod model is not able to describe the growth lag phase at the beginning of the experiments and after strong environmental perturbation during the cultivations [24, 25]. In order to deal with the growth lag phase, a metabolic regulator model [24] combined with the Monod model is used to describe the specific growth rate in this study. The model is finally validated with the experimental data of one batch culture and two fed-batch cultures with pulse feeding of nutrients.

Materials and methods

Cell line and culture medium

The myeloma cell line X63-Ag8.653, a non-secretor, was used in this study. The base medium used in flasks and spinners was RPMI 1640 supplemented with 10% fetal calf serum (FCS, Invitrogen, UK), 2 mM glutamine and 80 $\mu\text{g mL}^{-1}$ gentamicin. Two feeding mediums, FM1 and FM2, have the following composition: FM1 contains 18 g L^{-1} glucose and 3 g L^{-1} glutamine with 10 \times RPMI as base medium; FM2 contains 17.9 g L^{-1} glucose and 3.2 g L^{-1} glutamine with 1 \times RPMI as base medium. The composition of amino acids in RPMI 1640 medium is given in Table 1.

Inoculation preparation

Cells stored in liquid nitrogen were thawed and then cultured in the T-flasks. After subculturing in the T-flask with the area of 25 and 75 cm^2 , cells were transfer to the spinners for suspension culture with the culture volume of 50–500 mL. The viable cell densities for inoculation of flasks and spinners were 2.0×10^5 cells mL^{-1} and 3.0×10^5 cells mL^{-1} , respectively, and the final cell densities were 7.65×10^5 cells

Table 1 Amino acids concentrations in RPMI 1640

Amino acid	μM	Amino acid	μM
Asp	150.38	Tyr	160.22
Glu	136.05	Val	170.94
Asn	378.79	Met	100.67
Ser	285.71	Trp	24.51
Gln	2,054.79	Phe	90.91
His	96.77	Iso	381.68
Gly	133.33	Leu	381.68
Thr	168.07	Lys	273.97
Arg	1,390		

mL⁻¹ and 9.9×10^5 cells mL⁻¹, respectively, after the cultivation. In the subculture, temperature was maintained at 37 °C, while CO₂ concentration and humidity were controlled at 5 and 80%, respectively. Inocula were transferred to three 250 mL spinners for further experiments with the initial viable cell density of 1.5×10^5 cells mL⁻¹.

Cultivation procedures

All experiments started with a working volume of 150 mL, and the glucose and glutamine concentrations of 1.75 g L⁻¹ and 0.5 g L⁻¹, respectively.

Experiment 1: Batch culture without feeding.

Experiment 2: Fed-batch culture with one time feeding. FCS of 15 mL and 32 ml FM2 were added at 70 h to achieve the final glucose concentration of 4.0 g L⁻¹.

Experiment 3: Fed-batch culture with three times feeding. Three times medium feeding were carried out at 54.5, 73 and 113 h, respectively. Briefly, at 54.5 h, 2.5 mL FCS and 3.5 mL FM2 were added to achieve the final glucose concentration of 1.0 g L⁻¹. At 73 h, 8 ml FCS and 4 mL FM2 was added to achieve the final glucose concentration of 1.0 g L⁻¹. At 113 h, 13.6 mL supernatant was removed from the culture medium and then 10 mL FCS and 3.6 mL FM1 was added.

All experiments were stopped at 134 h. During the cultivation, the temperature was maintained at 37 °C, the agitation speed of the spinner is 120 rpm, while CO₂ concentration and humidity were controlled at 5 and 80%, respectively.

Analysis method

Cell density was determined by microscopic counting with a hemacytometer and the dead cells were evaluated by the trypan blue exclusion method. Glucose and lactate were measured with YSI2700 analyzer (Yellow Spring, OH, USA). Ammonia was measured by commercially available enzymatic kits (Boehringer Mannheim GmbH, FRG). Amino acids analysis was performed by OPA-derivatization followed by a reversed-phase HPLC column (KONTRON, Germany). The derivatives were monitored by fluorescence detector and output was recorded and analyzed by computer with Kroma2000 software.

Model development

Cell growth model

The dynamic balance of viable cells may be described as:

$$\frac{dX_v}{dt} = \mu X_v - \mu_d X_v - F_o X_v \tag{1}$$

where, X_v is the viable cell density; μ is the specific growth rate; μ_d is the specific death rate; V is the culture volume; F_o is the sampling flow rate. Therefore:

$$\frac{dX_v}{dt} = \mu X_v - \mu_d X_v - \left(\frac{dV}{dt} + F_o\right) \frac{X_v}{V} \tag{2}$$

Since:

$$\frac{dV}{dt} = F_i - F_o \tag{3}$$

with F_i as the feeding flow rate, Eq. (2) becomes:

$$\frac{dX_v}{dt} = \mu X_v - \mu_d X_v - \frac{F_i}{V} X_v \tag{4}$$

Similarly, the dynamic balance of dead cell density X_d is:

$$\frac{dX_d}{dt} = \mu_d X_v - k_{lys} X_d - \frac{F_i}{V} X_d \tag{5}$$

where k_{lys} is the specific autolysis rate. Then, the total cell density is

$$X_t = X_v + X_d \tag{6}$$

As stated in the introduction, glucose and glutamine limitation, ammonia and lactate accumulation and amino acid depletion should be considered in modeling. In our experiments, however, lactate and ammonia concentrations were less than 20 and 0.7 mM, which are much lower than the critical levels for cell growth inhibition, 40 mM for lactate and 5 mM for ammonia, respectively [18, 26]. Accordingly, they are not accounted for in modeling. Concentrations of amino acids during all experiments are depicted in Figs. 1, 2, 3, from which several amino acids were found exhausted during the cultivations. Among them, lysine concentration hit zero many times in all experiments. Therefore, lysine is modeled as a limiting amino acid. As found by Simpson et al. [22], there existed a short-term growth after deprivation of single amino acid. The amino acid demand during such a short-term growth period should be met with an intracellular amino acid pool [27]. Accordingly, the intracellular lysine concentration denoted by $C_{Lys-int}$ is finally used as a limiting substrate in modeling. Together with other substrates, the specific growth rate is firstly modeled with Monod kinetics:

$$\mu_M = \mu_{max} \frac{C_{Glc}}{C_{Glc} + K_{Glc}} \frac{C_{Gln}}{C_{Gln} + K_{Gln}} \frac{C_{Lys-int}}{C_{Lys-int} + K_{Lys-int}} \tag{7}$$

Using the specific growth rate described as Eq. (7), however, a much higher viable cell density is obtained than that of the measurement after inoculation or feeding, see the dash line in Fig. 4. Such a lag phase may result from the

Fig. 1 Time courses of essential amino acids in a batch culture (Exp.1), **a** limited and **b** unlimited

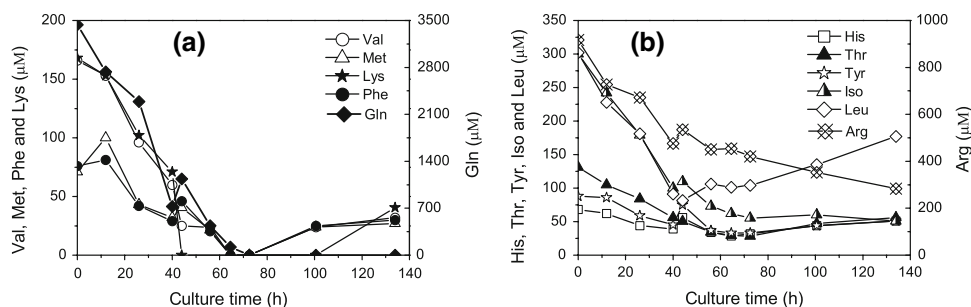


Fig. 2 Time courses of essential amino acids in a fed-batch culture (Exp.2), **a** limited and **b** unlimited. Arrows indicate feedings

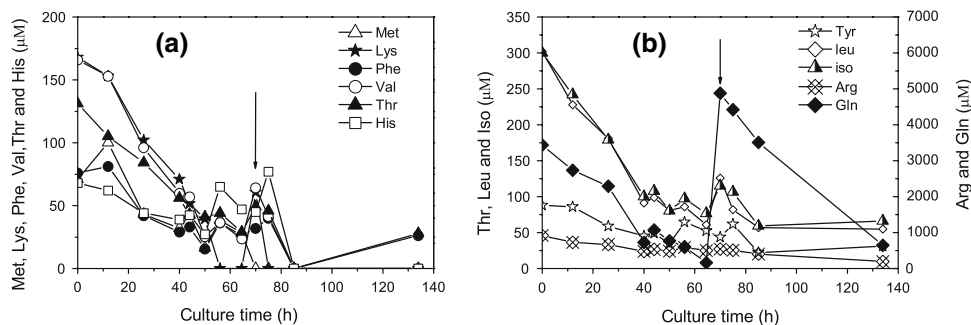
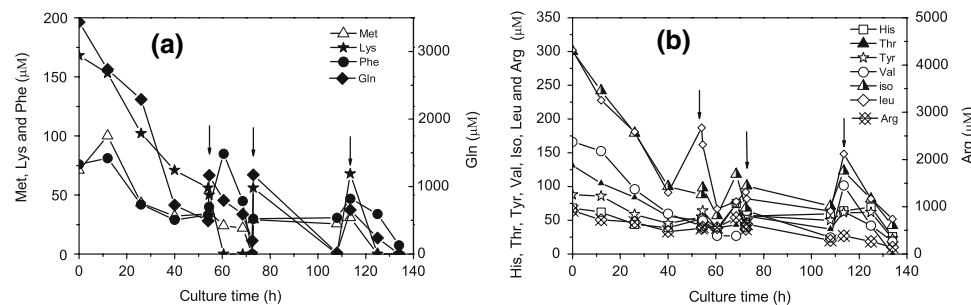


Fig. 3 Time courses of essential amino acids in a fed-batch culture (Exp.3), **a** limited and **b** unlimited. Arrows indicate feedings



low activity of enzyme pool responsible for intrinsic metabolism, such as glycolysis and glutaminolysis, shortly after inoculation or pulse feeding, see the “lag phase” in Figs. 7, 8, 9. To deal with the lag phase, a metabolic regulator model, proposed by Bellgardt [14, 28] is applied. The structure of the regulator model is illustrated in Fig. 5. The dashed frame outlines a first order regulator with μ as input and μ_R as output, which represents the actual activity of regulated pathway in analogy to enzyme levels of biochemical structure models. μ_{\min} stands for the minimum constitutive activity of the regulated pathway. k_1 and k_2 determine the transients of the lag phase. K is a low pass switch.

Figure 6 gives the transients of μ , the output of the regulator model (μ_R) and the output of the Monod type model (μ_M) for Exp.2 (pulse feeding is performed at 70 h). Shadow areas in Fig. 6, including part ‘A’, ‘B’, ‘C’ and ‘D’, indicate the difference between the output of Monod

model and the regulator model. The regulator model is structured to mimic the dynamics of the enzyme pool induction after substrate perturbation, while the Monod model can be thought as an indication of substrate level. After inoculation or feeding, the specific growth rate is limited by the low enzyme level, namely $\mu = \mu_R$, see part ‘A’ and ‘C’ in Fig. 6. When the enzyme is saturated, the specific growth rate is dependent on the substrate level, namely $\mu = \mu_M$, see part ‘B’ and ‘D’.

Mathematically, the regulator model is depicted with Eq. (8). The actual specific growth rate μ is obtained according to Eq. (9).

$$\frac{d\mu_R}{dt} = k_1(\mu + \mu_{\min}) - k_2\mu_R \quad (8)$$

$$\mu = \min\{\mu_M, \mu_R\} \quad (9)$$

The specific death rate μ_d is assumed to be determined by the specific growth rate [29–31], which is expressed as:

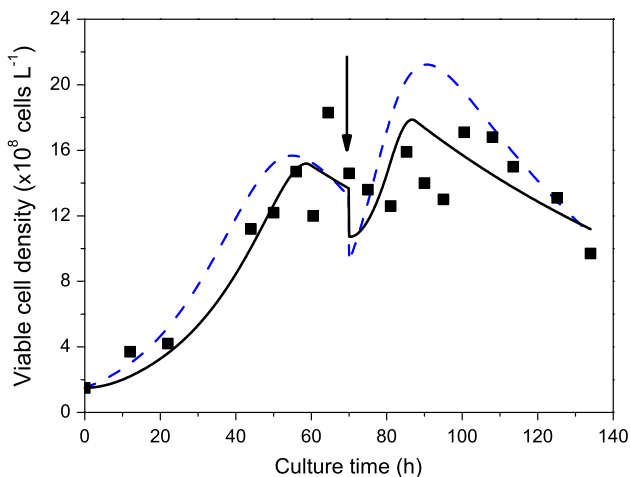


Fig. 4 Viable cell density simulated with the Monod model (dash line) and the combination of Monod model and regulator model (solid line), the experimental data from of Exp.2 (symbols). Arrow indicates the feeding

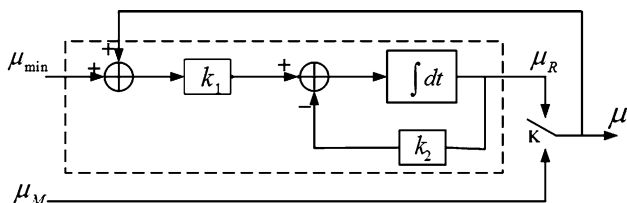


Fig. 5 Block diagram of the regulator model combined with the Monod model for the specific growth rate

$$\mu_d = \mu_{d,max} \frac{K_d}{\mu + K_d} \tag{10}$$

Mass balance model

Mass balance of glucose and glutamine are depicted with Eqs. (11) and (12), respectively, where the specific uptake rates are followed the Pirt linear model [32].

$$\frac{dC_{Glc}}{dt} = -q_{Glc}X_v + \frac{F_i}{V}(C_{Glc,F} - C_{Glc}) \tag{11}$$

$$\frac{dC_{Gln}}{dt} = -q_{Gln}X_v + \frac{F_i}{V}(C_{Gln,F} - C_{Gln}) \tag{12}$$

with

$$q_{Glc} = \begin{cases} \frac{\mu}{Y_{X/Glc}} + m_{Glc}, & C_{Glc} > 0 \\ 0, & C_{Glc} \leq 0 \end{cases} \tag{13}$$

$$q_{Gln} = \begin{cases} \frac{\mu}{Y_{X/Gln}} + m_{Gln}, & C_{Gln} > 0 \\ 0, & C_{Gln} \leq 0 \end{cases} \tag{14}$$

Lysine uptake is partitioned into two parts. One part is for cell growth and energy maintenance. In case of the

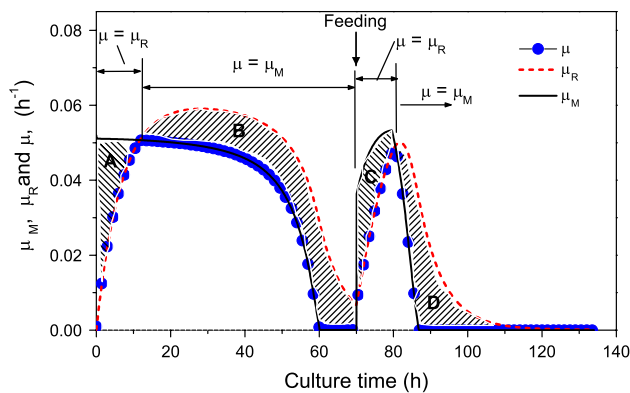


Fig. 6 The specific growth rate obtained from the Monod model (solid line), the regulator model (dashed line) and the combined model (filled circle) of Exp.2 (with pulse feeding added at 70 h)

intracellular lysine pool being less than the saturated value, another part of extracellular lysine is utilized to fill the intracellular pool. Therefore, the specific uptake rate of extracellular lysine can be described as:

$$q_{Lys-ext} = \begin{cases} \frac{\mu}{Y_{X/Lys}} + m_{Lys-ext} + f_{max} \frac{C_{Lys-int0} - C_{Lys-int}}{C_{Lys-int0} - C_{Lys-int} + K_f}, & C_{Lys-ext} > 0 \\ 0, & C_{Lys-ext} \leq 0 \end{cases} \tag{15}$$

where, $C_{Lys-int0}$ is the saturated level of intracellular lysine; f_{max} and K_f are model constants. The first two items on the right hand of Eq. (15) represent the lysine uptake for the cell growth and energy maintenance, respectively, while the other term is for filling the intracellular lysine pool. The uptake rate of extracellular lysine for filling the intracellular pool is assumed to be dependent on the difference between the saturated level and the actual intracellular lysine level. The mass balance of extracellular lysine is

$$\frac{dC_{Lys-ext}}{dt} = -q_{Lys-ext}X_v + \frac{F_i}{V}(C_{Lys-ext,F} - C_{Lys-ext}) \tag{16}$$

Intracellular lysine is used for cell growth and energy maintenance. The mass balance of intracellular lysine can be described as:

$$\frac{d(C_{Lys-int}v_0)}{dt} = q_{Lys-ext} - \left(\frac{\mu}{Y_{X/Lys}} + m_{Lys-ext} \right) \tag{17}$$

where v_0 is the single-cell volume, and it is assumed to be constant. The dynamics of the intracellular lysine concentration finally is

$$\frac{dC_{Lys-int}}{dt} = \begin{cases} \frac{1}{v_0}(q_{Lys-ext} - \frac{\mu}{Y_{X/Lys}} - m_{Lys-ext}), & C_{Lys-int} > 0 \\ 0, & C_{Lys-int} \leq 0 \end{cases} \tag{18}$$

Lactate is mainly produced by glucose metabolism. The specific production rate of lactate q_{Lac} is modeled as:

$$q_{\text{Lac}} = Y_{\text{Lac}/\text{Glc}} q_{\text{Glc}} \quad (19)$$

The mass balance of lactate concentration is:

$$\frac{dC_{\text{Lac}}}{dt} = q_{\text{Lac}} X_v - \frac{F_i}{V} C_{\text{Lac}} \quad (20)$$

Results and discussion

Three sets of experimental data, including the densities of total, viable and dead cells and concentrations of glucose, glutamine, extracellular lysine and lactate, from myeloma cell cultivations are used for model validation.

Nineteen parameters are involved in the model. Among them, saturated level of intracellular lysine $C_{\text{Lys_int0}}$ is assumed to be 0.1 g L^{-1} , about four times of the extracellular lysine level [21, 27, 33], and the specific autolysis rate k_{lys} is set to 0.0014 h^{-1} . Most of the model parameters, including the maximum specific growth/death rate, the saturated constants of the substrates, and the cell number yields from the substrates, are calculated directly by the batch experiment (Exp. 1). To minimizing the sum of square errors between the densities of viable and dead cells and the concentrations of glucose, glutamine, lysine and lactate from measurements and that from simulation results. The other parameters are identified by try and error. All the parameters used for model simulation of Exp. 1 are given in Table 2.

The sensitivity analysis of the model parameters is performed by using the method of Claes and Van Impe [34] and the data of Exp. 1. The objective function is the sum of the square error between measured (X_v^M) and simulated viable cell density (X_v^S), see Eq. (21), except for the lactate yield on glucose $Y_{\text{Lac}/\text{Glc}}$, whose objective function is the sum of the square error between measured (C_{Lac}^M) and simulated lactate concentration (C_{Lac}^S), see Eq. (22). Perturbation of each parameter by $\pm 10\%$ around the value listed in Table 2 is tested and the relative change of SSE is calculated. If the relative change of SSE caused by the perturbation exceeds $\pm 5\%$, the corresponding parameter is regarded as a sensitive one. It was found that five parameters are sensitive to perturbation and they are further identified by using Simplex method for all experiments while the other parameters take the fixed values in Table 2. The identified results are given in Table 3.

Table 2 Parameters used in the model

K_{Glc}	K_{Gln}	$K_{\text{Lys-int}}$	μ_{max}	$\mu_{\text{d,max}}$	K_{d}	μ_{min}	k_1	k_2	v_0
0.13	0.05	0.001	0.065	0.012	0.005	0.0001	0.18	0.15	4.3
$Y_{\text{X}/\text{Glc}}$	$Y_{\text{X}/\text{Gln}}$	$Y_{\text{X}/\text{Lys}}$	$Y_{\text{Lac}/\text{Glc}}$	m_{Glc}	m_{Gln}	$m_{\text{Lys-ext}}$	f_{max}	K_{f}	
10.5	45.0	750.0	0.80	0.00016	0.0004	0.000015	0.00005	0.02	

Units are referred to list of symbols

Table 3 Sensitive parameters for Exps. 1–3

Experiment	μ_{max}	$\mu_{\text{d,max}}$	$Y_{\text{X}/\text{Gln}}$	m_{Gln}	$Y_{\text{Lac}/\text{Glc}}$
1	0.065	0.012	45.0	0.0004	0.80
2	0.063	0.010	50.8	0.0005	0.85
3	0.060	0.011	46.0	0.0003	0.82

Units are referred to the list of symbols

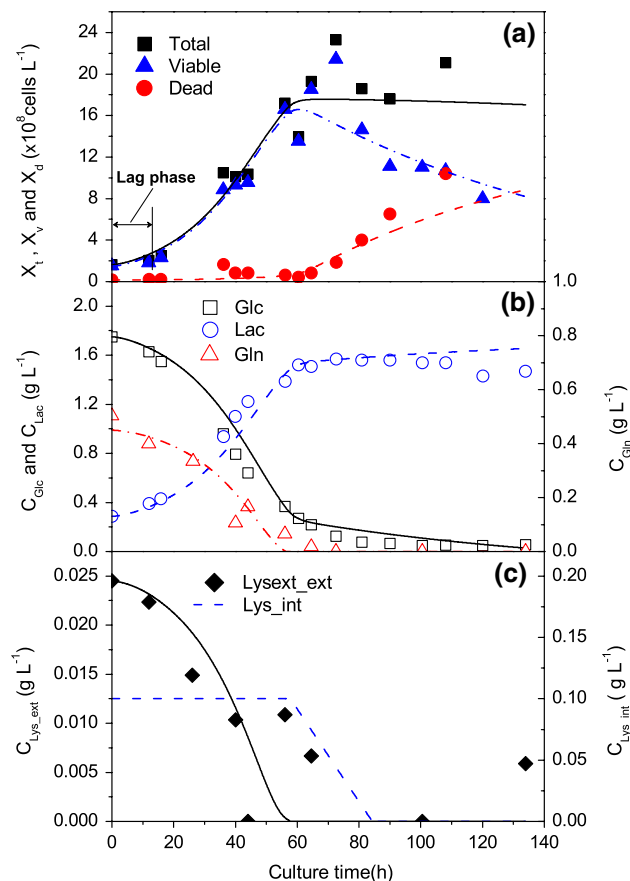


Fig. 7 Time courses of Exp. 1. **a** Total, viable and dead cell densities, **b** glucose, glutamine and lactate concentrations and **c** extra and intracellular lysine concentrations. Lines model simulations; symbols measurements

$$\text{SSE}_V = \sum_{i=1}^{12} \left[\frac{X_v^S(t_i) - X_v^M(t_i)}{X_v^M(t_i)} \right]^2 \quad (21)$$

$$\text{SSE}_{\text{Lac}} = \sum_{i=1}^{16} \left[\frac{C_{\text{Lac}}^S(t_i) - C_{\text{Lac}}^M(t_i)}{C_{\text{Lac}}^M(t_i)} \right]^2 \quad (22)$$

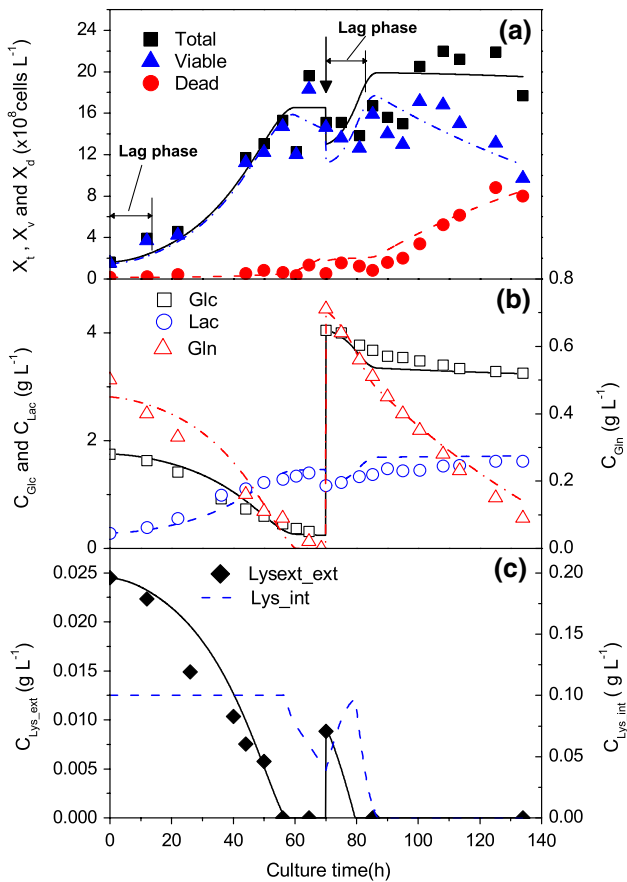


Fig. 8 Time courses of Exp. 2. **a** Total, viable and dead cell densities (arrow indicates the feeding), **b** glucose, glutamine and lactate concentrations and **c** extra and intracellular lysine concentrations. Lines model simulations; symbols measurements

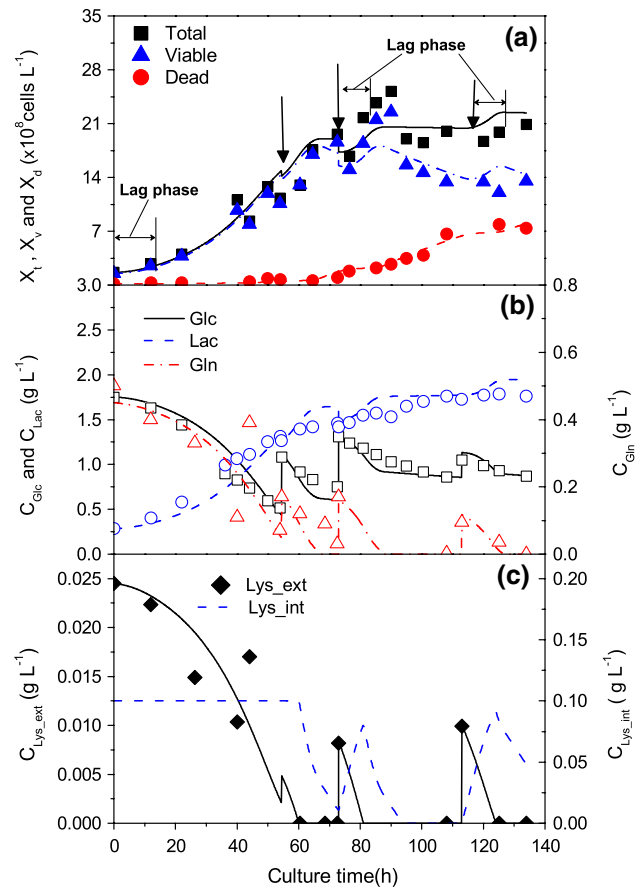


Fig. 9 Time courses of Exp. 3. **a** Total, viable and dead cell densities (arrows indicate the feeding), **b** glucose, glutamine and lactate concentrations and **c** extra and intracellular lysine concentrations. Lines model simulations; symbols measurements

Comparison between the simulation results and measurements are shown in Figs. 7, 8, 9. Figure 7 shows the time courses of Exp. 1, a traditional batch culture without feeding. According to model simulation, extracellular lysine support cell growth for about 57 h until the intracellular lysine consumption is triggered and lasts for about another 24 h, as was found to be 15 h in Simpson’s work [22]. The dynamics of intracellular lysine concentration is qualitatively coincident with the observation of Baydoun et al. [35]. Time courses of Exp. 2 are depicted with Fig. 8. Cell growth and cell metabolism similar to Exp. 1 are found before 70 h. Lysine was supplemented at 70 h by pulse feeding. However, it was soon exhausted at about 80 h. Figure 9 shows the comparison between simulation results and the experimental data of Exp. 3, in which three times of feeding medium were added at 54.5, 73 and 113 h, respectively. Cells switched from utilizing extracellular lysine to using lysine from an intracellular pool at 81 and 123 h after the second and third feedings, respectively.

The regulator model works well for the specific growth rate in these experiments. It operates at the beginning of the experiments and the short-term period after pulse feeding, as indicated with a “lag phase” in Figs. 7, 8, 9. In Exp. 1, the regulator model keeps on working until 12.4 h, when the specific growth rate is low with rich nutrients. After that, the Monod model takes the work over. In Exp. 2, the regulator model operates twice. The first one is similar to that of Exp. 1, and the second one operates from 70 to 82 h. In Exp. 3, the regulator model operates during the following periods, 0–12.5, 73–83 and 113–123.5 h, respectively. There is no lag phase after the first feeding at 54.5 h because the enzyme level is high enough to supply the maximum specific growth rate.

In the model presented above, only lysine is taken into account as the sole growth limiting amino acid. In fact, other essential amino acids, such as *methionine*, can be also exhausted during the cultivations, see Figs. 1, 2, 3. However, lysine was exhausted much earlier than the other amino acids. For simplicity, lysine limitation is regarded to

represent the lumped effect of other possible amino acids limitation.

Conclusions

A simple kinetic model has been developed for simulating the growth of myeloma cell line. Metabolic regulator model is used to describe the lag phase at the beginning of the cultivation or after feeding. Lysine is taken into account as a limiting substrate. Intracellular lysine acts as growth a limiting substrate when extracellular lysine is depleted. The dynamics of total, viable and dead cell densities and concentrations of glucose, glutamine, extra and intracellular lysine and lactate are described in this model. The model is validated with one batch culture and two batch cultures with pulse feeding.

It is noted that the simple kinetic model proposed in this paper was only validated with the experimental data with no expression of recombinant proteins. If the product expression is accounted for, the model has to be extended by incorporating the corresponding kinetics. The product formation rate may be determined by specific growth rate, death rate or substrate concentrations [3, 17]. Besides, substrate, especially amino acids, uptake in accordance with product formation should be modeled, which may have more straightforward model forms [5, 36, 37]. In summary, the simple kinetic model presented here provides a framework for further modeling studies which is more application oriented.

Acknowledgments The authors gratefully acknowledge the financial support of the Natural Science Foundation of China (Grant No. 60574038 and 20576136), the German DAAD Academic Visiting Scholarship (J. X. Bi), and the DFG/Germany-MOE/China Exchange Program (J. Q. Yuan). GBF (Gesellschaft fuer Biotechnologische Forschung GmbH, now called Helmholtz Zentrum für Infektionsforschung) is acknowledged for providing all experimental and analysis facilities. We sincerely thank Mrs. Angela Walter/GBF and Mr. Joachim Hammer/GBF for the analytical assistances.

References

- Glacken MW, Huang AJ (1989) Mathematical descriptions of hybridoma culture kinetics: III. Simulation of fed-batch bioreactor. *J Biotechnol* 10:39–66
- Frame KK, Hu WW (1991a) Kinetic study of hybridoma cell growth in continuous culture, I. A model for non-producing cells. *Biotechnol Bioeng* 37:55–64
- Zeng AP (1996) Mathematical modeling analysis of monoclonal antibody production by hybridoma cells. *Biotechnol Bioeng* 50:238–247
- Batt CB, Kompalla AK (1989) A structured modeling framework for the dynamics of hybridoma growth in continuous suspension cultures. *Biotechnol Bioeng* 34:515–531
- Sanderson CS, Barford JP, Barton GW (1999) A structured, dynamic model for animal cell culture systems. *Biochem Eng J* 3:203–211
- Ramkrishna D (2003) On modeling of bioreactors for control. *J Proc Cont* 13:581–589
- Namjoshi AA, Ramkrishna D (2005) A cybernetic modeling framework for analysis of metabolic systems. *Comp Chem Eng* 29:487–498
- Jang JD, Barford JP (2000) An unstructured kinetic model of macromolecular metabolism in batch and fed-batch cultures of hybridoma cells producing monoclonal antibody. *Biochem Eng J* 4:153–168
- Dhir S, Morrow KJ, Rhinehart RR, Wiesner T (2000) Dynamic optimization of hybridoma growth in a fed-batch bioreactor. *Biotechnol Bioeng* 67:197–205
- Ishii N, Robert M, Nakayama Y, Kanai A, Tomita M (2004) Toward large-scale modeling of the microbial cell for computer simulation. *J Biotechnol* 113:281–294
- Glacken MW, Adema E, Sinskey AJ (1988) Mathematical descriptions of hybridoma culture kinetics: I. initial metabolic rates. *Biotechnol Bioeng* 32:491–501
- de Tremblay M, Perrier M, Chavarie C, Archambault J (1992) Optimization of fed-batch culture of hybridoma cells using dynamic programming: single and multi feed case. *Bioproc Eng* 7:229–234
- Portner R, Schafer J (1996) Modeling hybridoma cell growth and metabolism—a comparison of selected models and data. *J Biotechnol* 49:119–135
- Zeng AP, Deckwer WD, Hu WS (1998) Determinants and rate laws of growth and death of animal cells in continuous cultures. *Biotechnol Bioeng* 57:642–654
- Gorman L, Mercer LP, Hennig B (1996) Growth requirements of endothelial cells in culture: variations in serum and amino acid concentration. *Nutrition* 12:266–270
- Marquis CP, Barford JP, Harbour C (1996) Amino acid metabolism during batch culture of a murine hybridoma AFP-27. *Cytotechnology* 21:111–120
- Heidemann R, Lutkemeyer D, Buntmeyer H, Lehmann J (1998) Effects of dissolved oxygen levels and the role of extra- and intracellular amino acid concentrations upon the metabolism of mammalian cell lines during batch and continuous cultures. *Cytotechnology* 26:185–197
- Simpson NH, Singh RP, Perani A, Goldenzon C, Al-Rubeai M (1998) In hybridoma cultures, deprivation of any single amino acid leads to apoptotic death, which is suppressed by the expression of the bcl-2 gene. *Biotechnol Bioeng* 59:90–98
- Martial-Gros AM, Goergen JL, Engasser JM, Marc A (2001) Amino acids metabolism by VO 208 hybridoma cells: some aspects of the culture process and medium composition influence. *Cytotechnology* 37:93–105
- Chen P, Harcum SW (2005) Effects of amino acid addition on ammonium stressed CHO cells. *J Biotechnol* 117:277–286
- Robert RS, Hsu H (1976) Amino acid metabolism of myeloma cells in culture. *J Cell Sci* 21:609–615
- Bree MA, Dhurjati P, Geoghegan RF (1988) Kinetic modelling of hybridoma cell growth and immunoglobulin production in a large-scale suspension culture. *Biotechnol Bioeng* 32:1067–1072
- Miller WM, Wilke CR, Blanch HW (1986) Kinetic analysis of hybridoma growth in continuous culture. ACS National Meeting, Anaheim
- Bellgardt KH (1983) Modellbildung des Wachstums von *Saccharomyces cerevisiae* in Rührkeselreaktoren, PhD Dissertation, University of Hannover
- Shoemaker J, Reeves GT, Gupta S, etc (2003) The dynamics of single-substrate continuous cultures: the role of transport enzymes. *J Theor Biol* 222:307–322
- Cruz HJ, Freitas CM, Alvers PM, Moreira JL, Carrondo MJT (2000) Effect of ammonia and lactate on growth, metabolism, and productivity of BHK cells. *Enzyme Microbial Technol* 27:43–52

27. Hod Y, Hershko A (1976) Relationship of the pool of intracellular valine to protein synthesis and degradation in cultured cells. *J Biol Chem* 251:4458–4467
28. Ren HT, Yuan JQ, Bellgardt KH (2003) Macrokinetic model for methylophilic *Pichia pastoris* based on stoichiometric balance. *J Biotechnol* 106: 53–68
29. Zhou F, Bi JX, Zeng AP, Yuan JQ A (2006) Macrokinetic and regulator model for myeloma cell culture based on metabolic balance of pathways. *Proc Biochem* 41:2207–2217
30. Sanderson CS, Barford JP, Barton GW (1999) A structured, dynamic model for animal cell culture system. *Biochem Eng J* 3:203–11
31. Zeng AP, Bi JX (2005) Cell culture kinetics and modeling. In: Ozturk SS, Hu W-S (eds) *Cell culture technology for pharmaceutical and cellular therapies*. Taylor and Francis Group, Atlanta, pp 299–347
32. Pirt SJ (1985) *Principles of microbe and cell cultivation*. Blackwell, Oxford
33. Lu SB, Sun XM, Zhang YX (2005) Insight into metabolism of CHO cells at low glucose concentration on the basis of the determination of intracellular metabolites. *Proc Biochem* 40:1917–1921
34. Claes JE, Van Impe JE (2000) Combining yield coefficients and exit-gas analysis for monitoring of the baker's yeast fed-batch fermentation. *Bioproc Eng* 22:195–200
35. Baydoun AR, Emery PW, Pearson JD (1990) Substrate-dependent regulation of intracellular amino acid concentrations in cultured bovine aortic endothelial cells. *Biochem Biophys Res Commun* 173:940–948
36. Frame KK, Hu WW (1991b) Kinetic study of hybridoma cell growth in continuous culture, II. Behavior of producers and comparison to non-producers. *Biotechnol Bioeng* 37:55–64
37. Bapat PM, Bhartiya S, Venkatesh KV, Wangikar PP (2006) Structured kinetic model to represent the utilization of multiple substrates in complex media during rifamycin B fermentation. *Biotechnol Bioeng* 93:779–790